Redox and UV/VIS/NIR spectroscopic properties of tris(pyrazolyl)borato–oxo–molybdenum(v) complexes with naphtholate and related co-ligands

Andrew M. McDonagh, Michael D. Ward* and Jon A. McCleverty*

School of Chemistry, University of Bristol, Cantock's Close, Bristol, UK BS8 1TS.
E-mail: mike.ward@bristol.ac.uk

Received (in London, UK) 23rd May 2001, Accepted 12th July 2001
First published as an Advance Article on the web 10th September 2001

A series of complexes has been prepared in which $\{(Tp^*)Mo^{V}(O)Cl\}^{+}$ termini [Tp* = tris(3,5-dimethylpyrazolyl) hydroborate] have been coordinated with ligands containing naphtholate binding sites. Mononuclear complexes, in which the sixth ligand is *e.g.* 1-naphtholate or 2-naphtholate, have been prepared; in addition some dinuclear complexes were also prepared based on bridging ligands containing either two naphtholate termini, or one naphtholate terminus and one phenolate terminus. The complexes have been studied by electrochemistry and UV/VIS/NIR spectroelectrochemistry to evaluate how the naphtholate donors affect the properties of the complexes compared to their known phenolate-based analogues. It was found that mononuclear complexes with phenolate, 1-naphtholate and 2-naphtholate ligands give significantly different electronic spectra in their oxidised [Mo(VI)] forms, with the characteristic phenolate → Mo(VI) LMCT transition being at much lower energy for the naphtholate complexes than the phenolate, an observation which is of significance for development of electrochromic near-IR dyes. In addition, the twist induced in some of the bridging ligands by the bulky naphtholate termini results in substantially decreased metal–metal electronic interactions compared to the equivalent phenolate-based complexes.

We have recently been interested in studying the electronic spectroscopic properties of mononuclear and dinuclear complexes containing $[(Tp^*)Mo^{V}(O)Cl(OAr)]$ or $[(Tp^*)Mo^{I}(NO)Cl(py)]$ fragments [Tp* = tris(3,5-dimethylpyrazolyl)hydroborate].[1–5] In the mononuclear complexes, the phenolate or pyridyl ligands are simple monodentate terminal ligands; in the dinuclear analogues, two such metal fragments are linked by bis-phenolate or bis-pyridyl bridging ligands respectively. Our interest in these was originally stimulated by the fact that both sets of dinuclear complexes show strong electronic and magnetic interactions between the metals, whose magnitude (and sign, in the case of magnetic exchange interactions) could be related to the structure of the bridging ligand.[1,2] During the course of these investigations we carried out UV/VIS/NIR spectroelectrochemical studies on many of the complexes, and it became apparent that some of them have the capacity to act as electrochromic near-IR dyes: that is, following a reversible one-electron redox process the complexes developed a strong charge-transfer transition in the near-IR region (800–1500 nm) which is completely absent when the redox process is reversed.[3–7] This is of some technological interest, as materials which display a near-IR switchable absorption can be used to modulate lasers which operate in this region of the spectrum, most notably for telecommunications applications.[8] Accordingly we have recently exploited the near-IR electrochromism of some of these complexes in a prototypical optical switching device.[7]

This paper specifically relates to mononuclear and dinuclear complexes of the type $[(Tp^*)Mo^{V}(O)Cl(OAr)]$, which were first reported by Enemark and co-workers[9] before being further exploited by us.[1–4] In the starting Mo(v) state the electronic spectrum is unremarkable, with the lowest-energy transition being a phenolate → Mo(v) ligand-to-metal charge-transfer (LMCT) in the visible region. These complexes can be reversibly oxidised to the Mo(VI) state and also reversibly reduced to the Mo(IV) state.[3,4,9] From spectroelectrochemical studies we found that on one-electron oxidation to $[(Tp^*)Mo^{VI}(O)Cl(OAr)]^{+}$, the lowest-energy LMCT transition [now phenolate → Mo(VI)] substantially increases in intensity and becomes red-shifted; this is the basis of the electrochromism which we have exploited in various dinuclear complexes.[3,4]

In this paper we wish to report the effect of changing the nature of the phenolate ligand (terminal for mononuclear complexes; bridging for dinuclear complexes) on the redox and electronic spectroscopic properties of a series of such complexes. In particular, we have found that replacing the single aromatic rings of phenolate donors with the fused bicyclic systems of naphtholate donors results in notable changes to these properties.

Results and discussion

Syntheses

The complexes described in this paper are listed in Scheme 1, together with some other relevant complexes which are included for comparison purposes. Complexes **1** and **2** are analogues of the parent mononuclear complex $[(Tp^*)Mo^{V}(O)Cl(OPh)]$,[9] but containing 1- or 2-naphtholate respectively in place of phenolate. Complex **3** is a derivative of **1** but with an extended conjugated azo-(4-methoxyphenyl) substituent. Complex **4** is a dinuclear analogue of **3**, arising from replacement of the methoxy group (of HL^3) by phenoxy (in H_2L^4) to create a second binding site; it is related to the known bis-phenolate complex **Mo(NN)Mo** which we described recently,[3] but with one phenolate terminus replaced by naphtholate. Complexes **5** and **6** are analogues of the dinuclear complex **Mo(th)Mo** which we also reported recently,[3]

 DOI: 10.1039/b104575j

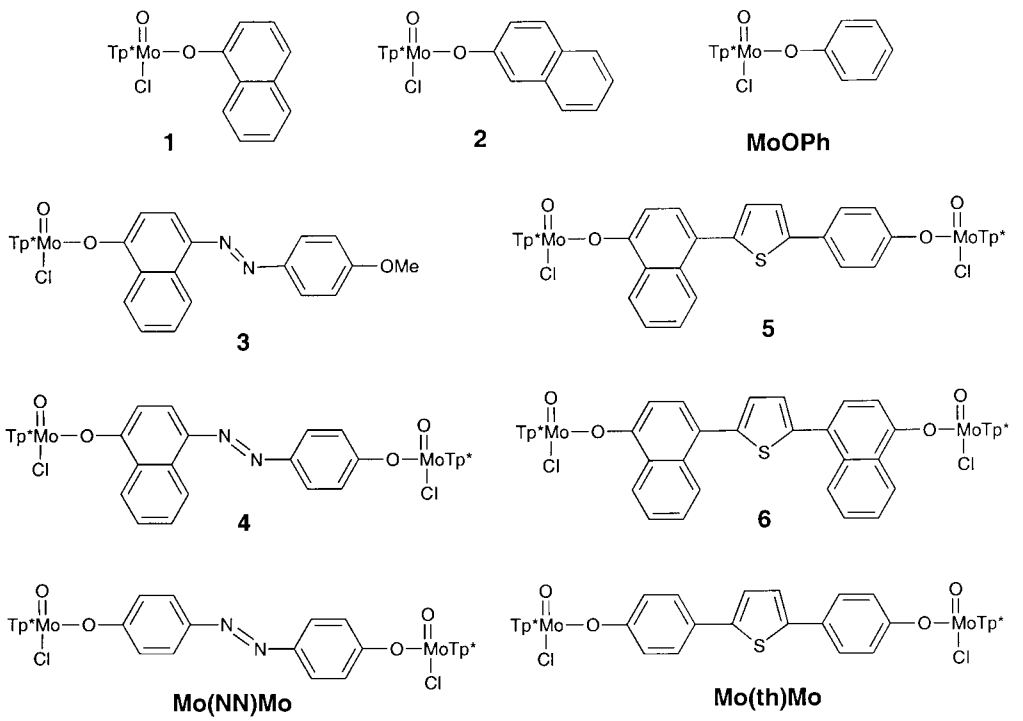

Scheme 1 Structural formulae of the complexes described in this paper.

but in which one (**5**) or both (**6**) of the phenolate termini are replaced by naphtholates.

The napthol–azo–phenol ligands used in complexes **3** and **4** (HL^3 and H_2L^4, respectively) were prepared by reaction of diazotised 4-methoxyaniline or 4-aminophenol with 1-naphthol using standard methods (Scheme 2).[10] We could not however prepare the symmetrical bis-naphthol ligand 4,4′-dihydroxy-1,1′-azonaphthalene (H_2L^a, Scheme 2), which is an obvious target for this work. Although the preparation of H_2L^a by diazotisation of 1-naphthol was reported a while ago,[11] the only characterisation data provided was a melting point. We repeated the reaction and found from the ^{1}H NMR spectrum of the product that it is actually 1,1′-dihydroxy-2,2′-azonaphthalene (H_2L^b, Scheme 2). The most obvious indication of this is that the chemical shift of the hydroxyl protons in $CDCl_3$ is 14.2 ppm, which arises from formation of O–H···N intermolecular hydrogen-bonds between the hydroxyl groups and the N atoms of the azo-bridge. Chemical shifts of this magnitude for phenolic OH groups are strongly diagnostic of such hydrogen-bonding,[12] which could not of course occur in H_2L^a, for which a 'normal' chemical shift of *ca.* 9–10 ppm for the phenolic proton would be expected. Formation of H_2L^b rather than H_2L^a is consistent with the earlier observation that 1-naphthol can readily diazotise at the 2-position;[11] in addition, formation of H_2L^b is no doubt facilitated by the formation of the two intermolecular O–H···N hydrogen bonds.

The unsymmetrical thiophene-bridged ligand used in complex **5** (H_2L^5) was prepared using the stepwise coupling procedure of Negishi.[13] Thus, reaction of 2-thienylzinc(II) bromide with 1-methoxy-4-iodonaphthalene in the presence of $[PdCl_2(PPh_3)_2]$ gave 1-methoxy-4-(2-thienyl)naphthalene (Scheme 3). This was then lithiated, treated with zinc(II) bromide, and reacted again under Negishi conditions with 4-iodoanisole to give the protected ligand precursor Me_2L^5. This reaction also produced as a by-product traces of the homo-coupled dimer 5,5′-bis(4-methoxynaphthyl)-2,2′-bithiophene (Scheme 3) which could be seen in the mass spectrum

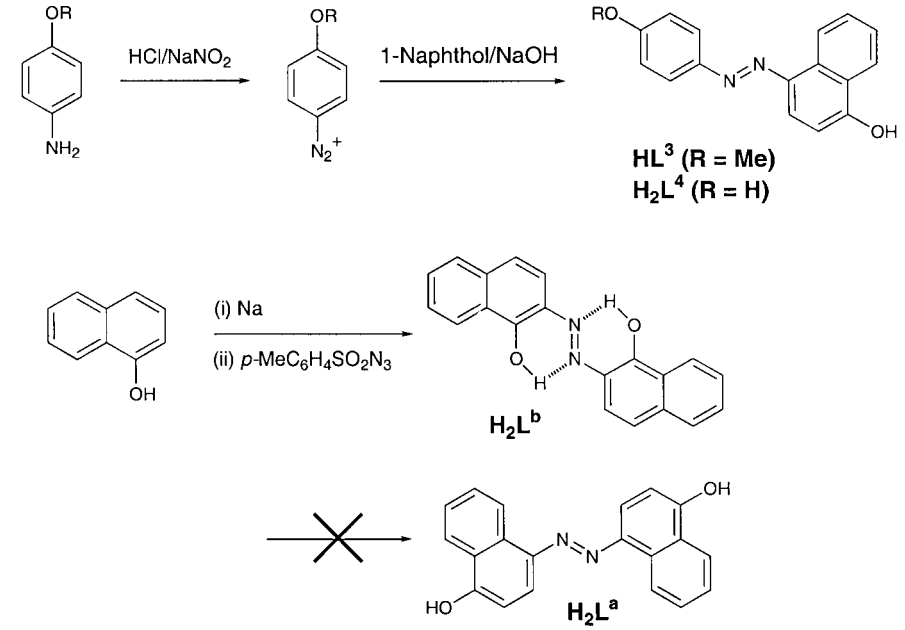

Scheme 2 Syntheses of HL^3 and H_2L^4, and the attempted synthesis of H_2L^a.

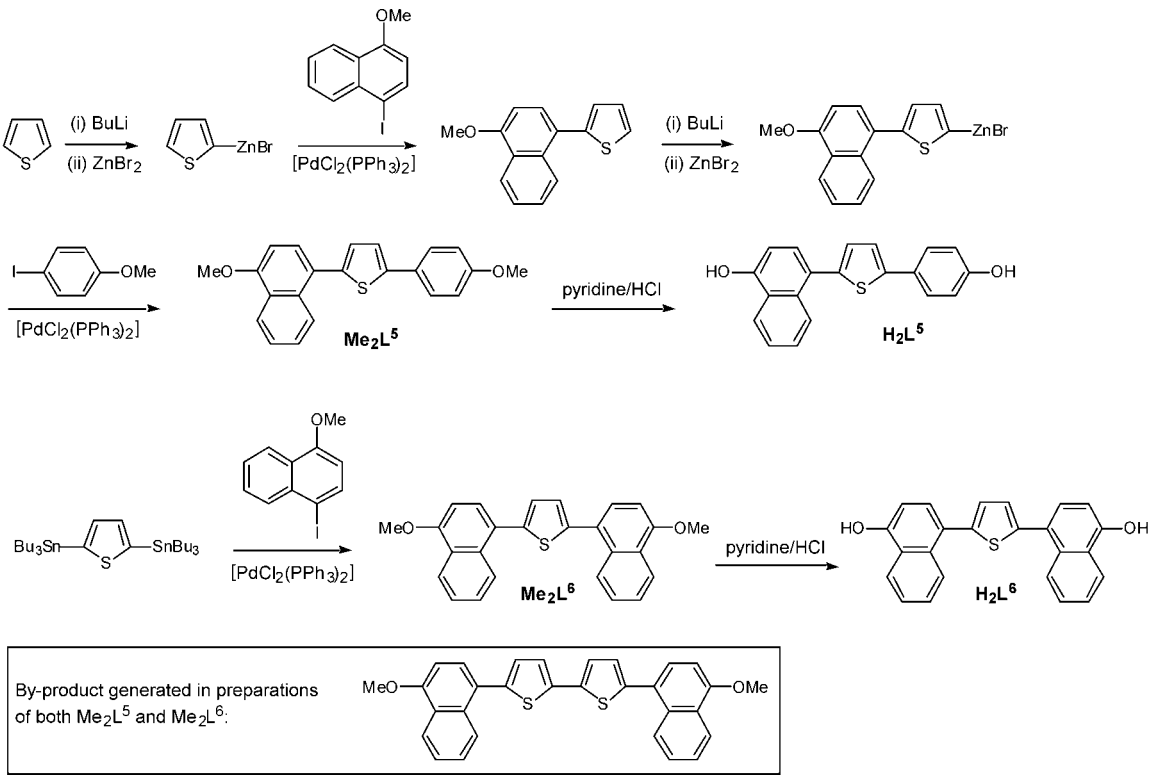

Scheme 3 Synthesis of H_2L^5 and H_2L^6.

(*m*/*z* 478). We could not separate this from Me_2L^5 by chromatography or recrystallisation, so the contaminated Me_2L^5 (*ca.* 95% pure by ^{1}H NMR) was used directly for deprotection (with pyridinium chloride) to give H_2L^5, and subsequent complex formation. We found that the unwanted dinuclear complex formed as a by product in this way *could* be separated satisfactorily by column chromatography from the desired complex **5** which was isolated analytically pure.

The symmetrical thiophene-bridged ligand with two naphthol termini, H_2L^6, was prepared using a Stille coupling procedure (Scheme 3) whereby $[PdCl_2(PPh_3)_2]$-catalysed coupling of 2,5-bis(tributylstannyl)thiophene with two equivalents of 1-methoxy-4-iodonaphthalene afforded Me_2L^6. As with synthesis of Me_2L^5, traces (*ca.* 5% compared to Me_2L^6) of 5,5′-bis(4-methoxynaphthyl)-2,2′-bithiophene were also produced and could not be separated from Me_2L^6. We therefore adopted the same procedure as with preparation of **5**, *viz.* demethylated the crude Me_2L^6 to give H_2L^6 which was used directly to prepare the dinuclear complex **6**. The trace of undesired dinuclear complex produced from coordination of 5,5′-bis(4-hydroxynaphthyl)-2,2′-bithiophene which is carried through could be separated chromatographically to give pure **6**.

All complexes were prepared by the same general route that has been described before.[2–4] Reaction of $[Mo^V(Tp^*)(O)Cl_2]$ (one or two equivalents per phenol unit in the ligand) with the deprotonated ligand in toluene at reflux, followed by purification by silica column chromatography, yielded the desired complexes in 23–60% yield. Characterisation data for the complexes are collected in Table 1. All complexes showed the expected molecular ion by FAB mass spectrometry, and also showed the characteristic B–H and Mo=O stretching vibrations in their IR spectra.

Electrochemical properties

Electrochemical data (determined by cyclic and square-wave voltammetry) for all of the complexes are collected in Table 2, together with data for related complexes from our earlier work for comparison purposes.

(i) Mononuclear complexes. Mononuclear complex **2** behaves as expected, showing reversible Mo(v)/Mo(vi) and Mo(iv)/Mo(v) couples at potentials similar to those of **MoOPh** [Fig. 1(a)]; the only difference is that the potential of the Mo(v)/Mo(vi) couple is *ca.* 50 mV less positive than that of **MoOPh**, *i.e.* 2-naphtholate stabilises the Mo(vi) state slightly more effectively than does phenolate. Complex **1** behaves rather differently: the Mo(iv)/Mo(v) couple is reversible, but at positive potentials the voltammogram shows two closely spaced processes of which the first (at +0.45 V *vs.* Fc/Fc^+) appears to be irreversible [Fig. 1(b)]. This behaviour does not change significantly on cooling the voltammetric cell to −30 °C. The presence of two processes suggests that one is metal-centred [Mo(v)/Mo(vi)] and the other is associated with

Table 1 Characterisation data for complexes **1**–**6**

Complex	Colour	Yield (%)	Elemental analytical data[a] (%)			IR[b]/cm^{-1}		FAB-MS
			C	H	N	ν_{BH}	ν_{MoO}	*m*/*z*
1	Green	60	51.6(51.1)	4.8(5.0)	13.8(14.3)	2546	947	589
2	Green	43	51.3(51.1)	4.3(5.0)	14.7(14.3)	2547	947	589
3	Brown	23	53.8(53.2)	4.8(4.8)	15.6(15.5)	2547	954	723
4	Black	27	47.9(48.0)	4.8(4.7)	16.7(17.0)	2543	951	1153
5	Green	44	49.5(49.8)	4.9(4.7)	13.7(13.9)	2547	947	1206
6	Green	33	51.9(51.7)	4.2(4.6)	12.9(13.4)	2548	951	1255

[a] Expected values in parentheses. [b] Compressed KBr pellets.

Table 2 Electrochemical data

Complex	$E_{1/2}$/V *vs.* Fc/Fc^+	
	Mo(IV)/Mo(V)	Other processes
MoOPh	−1.21	+0.68[b]
1	−1.21[a]	+0.45,[c] +0.68[d]
2	−1.21[a]	+0.70[b]
3	−1.07[a]	+0.49,[b] +0.82[d]
4	−1.15, −1.08	+0.40,[b] +0.63[e]
5	−1.17[a]	+0.30,[b] +0.58[e]
6	−1.14[a]	+0.32,[b] +0.46[e]
Mo(NN)Mo	−1.13[a]	+0.60,[b] +0.82[e]
Mo(th)Mo	−1.15[a]	+0.33,[b] +0.70[e]

[a] Two coincident, reversible, one-electron processes. [b] Reversible Mo(V)/Mo(VI) process. [c] Mo(V)/Mo(VI) process, electrochemically irreversible (see Fig. 1) but chemically reversible. [d] Irreversible, assumed to be ligand-centred. [e] Reversible ligand-centred process resulting in formation of bridging quinone (see text).

oxidation of the 1-naphtholate ligand; it is not obvious why **1** should behave differently from **2** and the other related mononuclear complexes. From the spectroelectrochemical results (see later) the first oxidation is metal-centred, so the second oxidation must be ligand-centred. Thus, replacement of phenolate by 1-naphtholate makes the Mo(V)/Mo(VI) couple considerably easier, as it shifts from +0.60 to +0.45 V *vs.* Fc/Fc^+.

Complex **3** also undergoes the expected reversible Mo(V)/Mo(VI) and Mo(IV)/Mo(V) couples, both of which occur at potentials closer to zero than for **MoOPh**; *i.e.* complex **3** both oxidises more easily and reduces more easily. It follows that these two processes cannot both be wholly metal-centred, because the effect of an electron-withdrawing or electron-donating substituent on the ligand would be to shift both redox potentials in the same direction. Some support for this is provided by the presence of a second (irreversible) oxidation at +0.82 V *vs.* Fc/Fc^+. The presence of the 4-methoxyphenyl unit on the naphtholate ligand means that double ligand-centred oxidation could be possible because a quinonoidal structure would result; we have observed this behaviour before in a series of complexes containing the $Mo^{VI}(=NAr)$ core.[14] Oxidation of these is irreversible, except when there is an additional amine unit in the 4-position, *i.e.* $Mo^{VI}(=NC_6H_4NMe_2)$: in this case two reversible, ligand-centred oxidations occur to generate a coordinated diiminobenzoquinone whose existence was confirmed by spectroelectrochemical methods.[14] We suggest that complex **3** is behaving similarly. The more modest potential of the reduction [the Mo(IV)/Mo(V) couple] compared to **MoOPh** indicates that the naphtholate ligand is a less effective electron donor than simple phenolate, in agreement with the presence of an electron-withdrawing azo substituent. The more modest first oxidation potential, and the presence of a second oxidation, suggest that the oxidation processes have more ligand-centred character in **3** than they do in **MoOPh** due to the possibility of a quinonoidal structure forming in the doubly oxidised state.

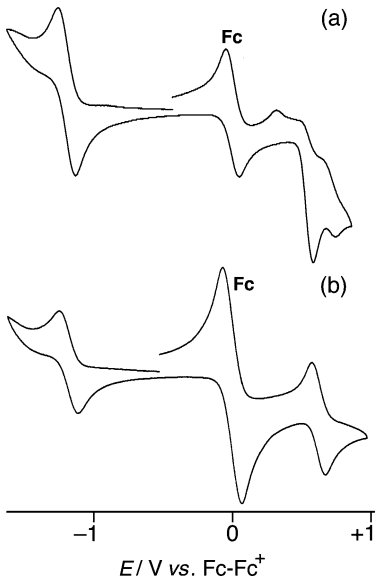

Fig. 1 Cyclic voltamograms of (a) **1** and (b) **2** in CH_2Cl_2 at a Pt-bead electrode (scan rate 0.2 V s^{-1}; Fc denotes the ferrocene/ferrocenium wave).

(ii) Dinuclear complexes. The dinuclear complexes show some interesting behaviour which is related to the conformation of the bridging ligands. The known complex **Mo(NN)Mo** undergoes two reversible Mo(V)/Mo(VI) processes which are separated by 220 mV; the two Mo(IV)/Mo(V) couples, at negative potential, are sufficiently close together that they cannot be resolved and a single double-intensity wave is seen in the voltammogram.[3] Similar behaviour is shown by **Mo(th)Mo**, although the separation between the Mo(V)/Mo(VI) couples is larger (370 mV).[3] The reasons for this have been discussed in detail,[3,4] but the important point for our purposes is that the separation ($\Delta E_{1/2}$) between the two Mo(V)/Mo(VI) couples is a measure of the electronic interaction between the two metal centres in the Mo(V)/Mo(VI) mixed-valence state, *i.e.* a measure of the ability of the bridging ligand to delocalise charge across it. It is clear that the thienyl bridging unit of **Mo(th)Mo** results in more effective delocalisation in the Mo(V)/Mo(VI) state than does the azo-linkage of **Mo(NN)Mo**.

Replacing one phenolate terminus of the bridging ligand in **Mo(NN)Mo** by a 1-naphtholate unit, to give complex **4**, has little effect on the electronic properties: the separation between the two Mo(V)/Mo(VI) redox couples increases marginally from 220 to 230 mV but this is at the limit of significance. Complexes **Mo(NN)Mo** and **4** have essentially identical metal–metal electronic interactions and the two bridging ligands behave in a very similar manner.

In contrast to this, repacement of phenolate by naphtholate units in the bridging ligand of **Mo(th)Mo** (to give complexes **5** and **6**) has a substantial effect on the electrochemical properties (Fig. 2). In complex **5** (one naphtholate terminus in the bridging ligand) the separation between the Mo(V)/Mo(VI) couples is reduced from 370 to 250 mV, and addition of the second naphtholate unit (in **6**) diminishes the redox separation still further, to 140 mV; *i.e.* a drop of roughly 40% in $\Delta E_{1/2}$ per replacement of phenolate by naphtholate. This can be ascribed to a conformational effect, *viz.* the greater dihedral

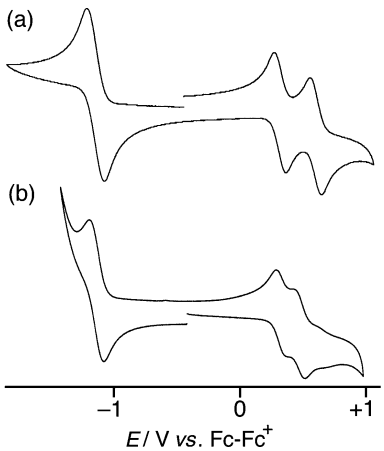

Fig. 2 Cyclic voltammograms of (a) **5** and (b) **6** in CH_2Cl_2 at a Pt-bead electrode (scan rate 0.2 V s^{-1}).

angles between naphtholate and thienyl groups in the bridging ligands of **5** and **6**, compared to the angles between the phenolate and thienyl groups in the bridging ligand of **Mo(th)Mo**. Energy-minimisation of the free bridging ligands in **Mo(th)Mo**, **5** and **6** using MOPAC (AM1 parameters) in Chem-3D[15] showed that the dihedral angle between the terminal phenol units and the central thienyl unit in 2,5-bis(4-hydroxyphenyl)thiophene [the bridging ligand of **Mo(th)Mo**] is *ca.* 26°. For H_2L^5 the phenol/thienyl dihedral angle is 27°, whereas the naphthol/thienyl dihedral angle is 55°; and in H_2L^6, both naphthol/thienyl dihedral angles are predicted to be between 50 and 60°. The greater cumulative twist between the component rings of the bridging ligands along this series of complexes will disrupt delocalisation between the metal centres in the mixed-valence Mo(v)/Mo(vi) state, resulting in the decreased redox separations that we observe. That such an effect is not operative in **4** is because the two-atom azo bridge has a much weaker steric interaction with the naphthol group; energy-minimisation of the structure of H_2L^4 in the same way results in a planar structure, indicating that the naphthol unit does not cause any distortions of the bridging ligand in **4**.

UV/VIS/NIR spectroelectrochemical studies

(i) Mononuclear complexes. It will be helpful at this point to reprise briefly the electronic spectroscopic behaviour of the parent mononuclear complex **MoOPh**.[4] In its starting oxidation state [Mo(v)] the lowest-energy electronic transition is a phenolate → Mo(v) LMCT process at 520 nm. On one-electron oxidation to the Mo(vi) state this is replaced by two more intense transitions, at 475 and 681 nm, which are both assigned as phenolate → Mo(vi) LMCT processes. In contrast, reduction of **MoOPh** to the Mo(iv) state results in collapse of the phenolate → Mo(v) LMCT transition.

For complex **1**, the lowest-energy LMCT transition is at 634 nm (*cf.* 520 nm for **MoOPh**). Oxidation to the Mo(vi) state at −30 °C resulted, as with **MoOPh**, in formation of two new more intense transitions at 1252 and 672 nm which are entirely characteristic of phenolate → Mo(vi) LMCT transitions (Table 3). Isosbestic points were maintained for the overlaid spectra as the oxidation progressed (Fig. 3), indicating a clean conversion between the starting Mo(v) state and the final Mo(vi) state, which we found surprising in view of the irreversibility of the first oxidation (even at −30 °C) by cyclic voltammetry. Reversing the applied potential resulted in regeneration of the starting Mo(v) spectrum with no significant decomposition. It follows that this first oxidation is chemically reversible even though it is electrochemically irreversible. However, increasing the potential beyond the point where the first oxidation is complete results in rapid decomposition of the complex. It follows that the second (presumably ligand-centred) process is completely chemically irreversible.

Apart from the reversibility of the process, comparison of the spectra of $[\mathbf{1}]^+$ and $[\mathbf{MoOPh}]^+$ is interesting. Replacement of phenolate by 1-naphtholate results in a substantial red-shifting of the lowest-energy LMCT transition in the Mo(vi) form of the complex (from 681 to 1252 nm). This is significant, because the 1200–1500 nm region of the near-IR spectrum is the part which is of interest for transmitting information along silica fibre-optic cables: a simple substitution of a monodentate ligand has resulted in the electrochromic behaviour of **1** shifting into exactly the region which is of technological interest. As with **MoOPh**,[4] one-electron reduction to the Mo(iv) state results in disappearance of the phenolate → Mo(v) LMCT transition, giving a spectrum with no significant absorbance at wavelengths longer than about 500 nm apart from a very weak (barely detectable) Mo(iv)-based d–d transition at *ca.* 800 nm.

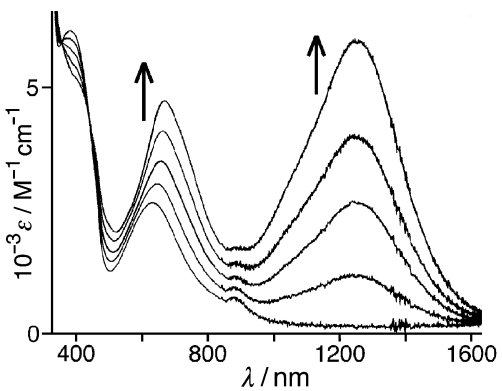

Fig. 3 Electronic spectra recorded during oxidation of **1** to $[\mathbf{1}]^+$ in an OTTLE cell (CH_2Cl_2, 243 K).

Table 3 Spectroelectrochemical data (CH_2Cl_2, 243 K)

Complex	λ_{max}/nm ($10^{-3}\varepsilon$/dm^3 mol^{-1} cm^{-1})			
1	634(2.2)	392(5.6)	316(11)	273(11)
$\mathbf{1}^+$	1252(7.3)[a]	672(4.6)[a]	308(10)	275(10)
$\mathbf{1}^-$	422(2.1)	364(6.3)	324(7.7)	
2	591(2.7)	265(17)		
$\mathbf{2}^+$	1457(0.9)[a]	644(3.8)[a]		
$\mathbf{2}^-$	323(9.6)	300(9.6)		
3	707(3.1)	432(23)	270(20)	
$\mathbf{3}^+$	948(20)[a]	656(33)	311(14)	
$\mathbf{3}^-$	860(3.1)	631(7.9)	487(19)	288(14)
4	452(24)	259(31)		
$\mathbf{4}^+$	947(29)[a]	483(9.2)[a]	255(26)	
$\mathbf{4}^{2+}$	444(29)	378(31)[b]		
$\mathbf{4}^{2-}$	801(5)	542(20)	339(11)	
5	667(7.2)	335(26)		
$\mathbf{5}^+$	1202(32)[a]	722(23)[a]	475(10)	423(10)
$\mathbf{5}^{2+}$	813(44)	702(79)[b]	433(13)	308(19)
$\mathbf{5}^{2-}$	373(26)			
6	680(6.4)	337(26)		
$\mathbf{6}^+$	1396(35)[a]	767(22)[a]	333(20)	
$\mathbf{6}^{2+}$	741(63)[b]	435(13)		
$\mathbf{6}^{2-}$	382(24)			

[a] Phenolate → Mo(vi) LMCT. [b] Predominantly ligand-centred transition associated with bridging quinone; see ref. 3.

Complex **2** (with a 2-naphtholate ligand) behaves significantly differently. In the starting Mo(v) state, the phenolate → Mo(v) LMCT is at 591 nm. On oxidation to the Mo(vi) state the two new phenolate → Mo(vi) LMCT transitions are now at 1457 and 644 nm, with the 1457 nm transition being of much lower intensity than the corresponding transition in $[\mathbf{1}]^+$ and $[\mathbf{MoOPh}]^+$ ($\varepsilon = 900$ M^{-1} cm^{-1}, compared to values of ≈10 000 M^{-1} cm^{-1} for $[\mathbf{1}]^+$ and $[\mathbf{MoOPh}]^+$). The behaviour of **2** on reduction to the Mo(iv) state is however similar to that of **1** and **MoOPh**.

For complex **3**, one-electron oxidation to the Mo(vi) state results in appearance of the two phenolate → Mo(vi) LMCT transitions at 656 and 948 nm (Fig. 4). The effect of the methoxyphenyl–azo substituent therefore, compared to complex $[\mathbf{1}]^+$, is to increase the energy of the LMCT transitions (consistent with the substituent having a net electron-withdrawing effect, which will increase the HOMO–LUMO gap) and also to increase their intensity.

(ii) Dinuclear complexes. The spectroelectrochemical properties of **Mo(NN)Mo** and **Mo(th)Mo** have been described recently and the details for these are included in Table 3.[3] Briefly, in each case one-electron oxidation to the mixed-valence Mo(v)/Mo(vi) state resulted in appearance of an intense near-IR transition at 1268 nm (for $[\mathbf{Mo(NN)Mo}]^+$) and 1199 nm (for $[\mathbf{Mo(th)Mo}]^+$), which we assigned as phenolate → Mo(vi) LMCT transitions associated with the Mo(vi) terminus. However, the second oxidation resulted in

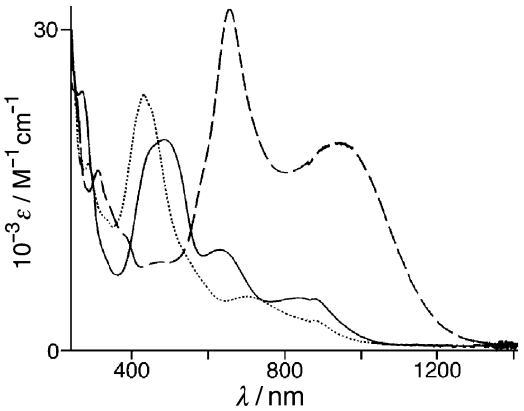

Fig. 4 Electronic spectra of **3** (dotted line), $[\mathbf{3}]^+$ (dashed line) and $[\mathbf{3}]^-$ (solid line) (CH_2Cl_2, 243 K).

collapse of the LMCT transition in each case and appearance of an intense transition at higher energy (409 and 684 nm respectively), which we believe to be associated with formation of a bridging quinone, arising from double ligand-centred oxidation. Thus, the first oxidation is metal-centred to give a Mo^{V}(μ-diolate)Mo^{VI} species, but the second oxidation results in an internal charge redistribution to give a species best described (on the basis of electronic spectra) as Mo^{V}(μ-quinone)Mo^{V}, in agreement with the known ability of extended bis-phenolates to oxidise in this way.

Complex **4** behaves generally similarly to **Mo(NN)Mo**. On one-electron oxidation to the Mo(V)/Mo(VI) state $[\mathbf{4}]^+$, an intense, low-energy absorption appears centred at 947 nm with $\varepsilon = 29\,000\ M^{-1}\ cm^{-1}$ (Fig. 5). The 947 nm LMCT transition consists of several closely-spaced components (separation *ca.* 1300 cm^{-1}) which we assume to be due to vibrational fine-structure. On further oxidation to $[\mathbf{4}]^{2+}$ this

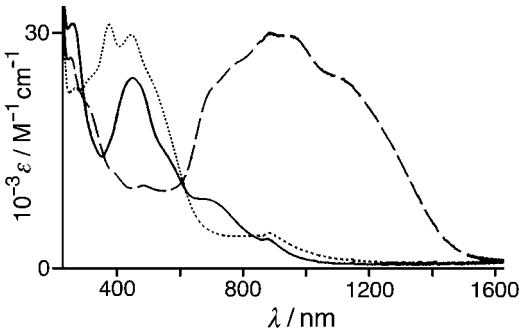

Fig. 5 Electronic spectra of **4** (solid line), $[\mathbf{4}]^+$ (dashed line) and $[\mathbf{4}]^{2+}$ (dotted line) (CH_2Cl_2, 243 K).

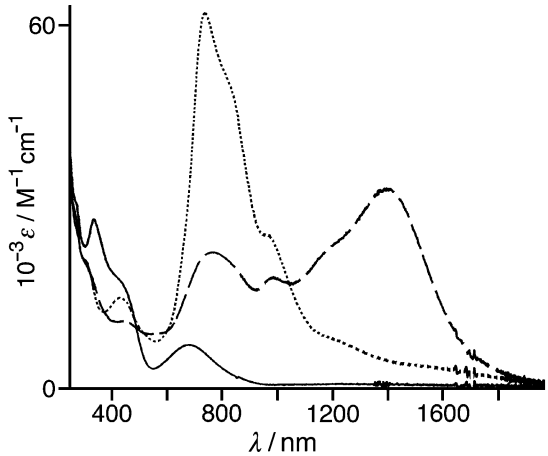

Fig. 6 Electronic spectra of **6** (solid line), $[\mathbf{6}]^+$ (dashed line) and $[\mathbf{6}]^{2+}$ (dotted line) (CH_2Cl_2, 243 K).

disappears and is replaced by a pair of higher-energy transitions at 444 and 378 nm, which we assume (following our earlier work)[3] to be ligand-centred processes associated with formation of a bridging quinone.

Complex **5** likewise behaves comparably to **Mo(th)Mo**, although the effects of successive replacement of phenolate by naphtholate are evident. On one-electron oxidation of **5** to the Mo(V)/Mo(VI) species, phenolate → Mo(VI) LMCT transitions which occur at 1199 and 673 nm for $[\mathbf{Mo(th)Mo}]^+$ are observed at 1202 and 722 nm for $[\mathbf{5}]^+$, *i.e.* very little change in the position of the peak maxima. The implication of this is that in this asymmetric complex it is the Mo–phenolate terminus which oxidises first, and not the Mo–naphtholate, such that the spectrum of oxidised $[\mathbf{5}]^+$ looks very similar to that of $[\mathbf{Mo(th)Mo}]^+$ because phenolate → Mo(VI) transitions are involved in each case. On further oxidation to $[\mathbf{5}]^{2+}$, these LMCT transitions are again replaced by a sharper transition at higher energy (702 nm, with a shoulder at 813 nm; *cf.* 684 and 845 nm for $[\mathbf{Mo(th)Mo}]^{2+}$) ascribable to quinone formation in the bridging ligand.[3]

Complex **6** shows significantly different behaviour. The naphtholate → Mo(VI) LMCT transitions in $[\mathbf{6}]^+$ occur at 1396 and 767 nm (Fig. 6); these are considerably red-shifted compared to the related phenolate → Mo(VI) LMCT transitions of $[\mathbf{5}]^+$ and $[\mathbf{Mo(th)Mo}]^+$, which reflects the comparative behaviour of $[\mathbf{1}]^+$ and $[\mathbf{MoOPh}]^+$ [naphtholate → Mo(VI) LMCT transition at 1252 nm in the former; phenolate → Mo(VI) LMCT transition at 681 nm in the latter]. The bridging quinone arising from the second oxidation to give $[\mathbf{6}]^{2+}$ has its absorption maximum at 741 nm. The steady shift in the position of this transition (684, 702 and 741 nm for $[\mathbf{Mo(th)Mo}]^{2+}$, $[\mathbf{5}]^{2+}$ and $[\mathbf{6}]^{2+}$ respectively) is consistent with the more extended delocalised networks that will occur in the bridging quinone units as phenol termini are relaced by naphthol termini.

Conclusions

Compared to the known mononuclear and dinuclear complexes of this type, changing the phenol terminus to naphtholate results in some significant differences in electrochemical and spectroscopic behaviour. In the mononuclear complexes, **MoOPh**, **1** and **2** (with phenolate, 1-naphtholate and 2-naphtholate as ligands) show variations in behaviour ascribable to the electronic properties of the ligands. In particular, $[\mathbf{1}]^+$ and $[\mathbf{2}]^+$ display LMCT transitions which are strongly red-shifted compared to those of $[\mathbf{MoOPh}]^+$, with that of $[\mathbf{1}]^+$ being much more intense than that of $[\mathbf{2}]^+$. In the dinuclear complexes, steric effects are apparent in complexes **5** and **6** arising from the greater degree of twist in the bridging ligand imposed by the bulky naphtholate units; this has the effect of reducing the metal–metal electronic interaction as the bridging ligand becomes more twisted.

Experimental

General

All reactions were performed under a nitrogen atmosphere using pre-dried solvents unless otherwise stated. $[Mo(Tp^*)(O)Cl_2]$,[9] $[PdCl_2(PPh_3)_2]$,[16] 1-methoxy-4-iodonaphthalene,[17] and 2,5-bis(tri-*n*-butylstannyl)thiophene[18] were prepared according to published methods. 1-Naphthol (BDH), 2-napthol (Acros), 4-methoxyaniline (Avocado), 4-aminophenol (Aldrich), thiophene (Aldrich) and 4-iodoanisole (Lancaster) were used as received.

Mass spectra were recorded using a VG Autospec instrument. Infrared spectra were recorded from compressed KBr

pellets using a Perkin-Elmer 1600 FT-IR. UV-Vis spectra were recorded using a Perkin-Elmer Lambda 2 spectrophotometer. ^{1}H NMR spectra (270 MHz) were recorded using a JEOL GX-270 NMR spectrometer and are referenced to internal $SiMe_4$. Electrochemical measurements were recorded on an EG&G/PAR model 273 potentiostat using a standard three-electrode configuration consisting of Pt bead working and auxiliary electrodes and a silver wire pseudo-reference electrode; all measurements were calibrated against internal ferrocene, and potentials are quoted against the ferrocene/ferrocenium couple (Fc/Fc^+). Solutions for electrochemical studies in dry CH_2Cl_2 contained 0.1 M $[NBu^n_4]PF_6$ as base electrolyte, and were *ca.* 1 mM in analyte. Spectroelectrochemical measurements were performed at 243 K in a home-built OTTLE cell using a Perkin-Elmer Lambda 19 spectrophotometer, as previously described.[14]

Syntheses of ligands

4-Hydroxy-1-[4-(methoxyphenyl)azo]napthalene (HL^3). 4-Methoxyaniline (0.89 g, 7.2 mmol) was added to a solution of conc. hydrochloric acid (2.6 cm^3) in water (2.6 cm^3) and then cooled to 0 °C in a salt/ice bath. A solution of sodium nitrite (0.54 g, 7.8 mmol) in water (3 cm^3) was then added slowly with stirring ensuring the temperature did not rise above 5 °C. In a separate flask, 1-naphthol (1.4 g, 9.7 mmol) was dissolved in a solution of sodium hydroxide (1.6 g) in water (10 cm^3) and the mixture cooled in an ice bath. To this was slowly added the diazonium salt with stirring. After stirring for 15 min, conc. hydrochloric acid (5 cm^3) was added. The crude product was then collected by filtration and purified by silica column chromatography eluting with a 1 : 1 hexane–diethyl ether mixture. Yield was 0.99 g (49% based on 4-methoxyaniline). EI MS: m/z 278 (M^+, 100%), 143 ($[HOC_{10}H_6]^+$, 90%). ^{1}H NMR (270 MHz, $(CD_3)_2CO$): δ 3.92 (3H, s; Me), 7.06 (1H, d, $J = 8$; naphthyl), 7.14 (2H, d, $J = 8$; phenyl), 7.57–7.72 (2H, m; napthyl), 7.88 (1H, d, $J = 8$; naphthyl), 8.01 (2H, d, $J = 10$; phenyl), 8.34 (1H, d, $J = 8$; naphthyl), 8.99 (1H, d, $J = 10$ Hz, naphthyl), 9.76 (1H, br s, OH).

4-Hydroxy-1-[4-(hydroxyphenyl)azo]naphthalene (H_2L^4). Using the same procedure as above, 4-aminophenol (1.0 g, 9.2 mmol) and 1-naphthol (1.4 g, 9.9 mmol) gave 1.5 g (60%) of the desired product. EI MS: m/z 264 (M^+, 75%), 143 ($[HOC_{10}H_6]^+$, 100%). ^{1}H NMR (270 MHz, $(CD_3)_2CO$): δ 7.04 (3H, m; phenyl and naphthyl), 7.56–7.71 (2H, m; naphthyl), 7.85 (1H, d, $J = 8$; naphthyl), 7.94 (2H, d, $J = 9$; phenyl), 8.33 (1H, d, $J = 9$; naphthyl), 8.98 (1H, d, $J = 8$ Hz; naphthyl), 9.02 (1H, br s, HOC_6H_4), 9.93 (1H, br s, $HOC_{10}H_6$).

1-Methoxy-4-(2-thienyl)naphthalene. Thiophene (0.40 g, 4.8 mmol) was dissolved in tetrahydrofuran (25 cm^3) and cooled to −40 °C (dry ice/acetonitrile bath), and *n*-BuLi (4.8 mmol; 3.0 cm^3 of a 1.6 M solution in hexane) was added dropwise. The mixture was stirred at −40 °C for 45 min and then added to a solution of dry zinc(II) bromide (1.07 g, 4.8 mmol) in tetrahydrofuran (15 cm^3) at 0 °C. This mixture was stirred at 0 °C for 1 h and then added to a solution of 1-methoxy-4-iodonaphthalene (1.0 g, 3.5 mmol) and $[PdCl_2(PPh_3)_2]$ (0.145 g, 0.21 mmol) in tetrahydrofuran (30 cm^3) at room temperature. After stirring for 2.5 h at room temperature, the solvent was removed using a rotary evaporator and the residue purified by column chromatography on silica eluting with a 1 : 4 dichloromethane–hexane mixture. The second band was collected and yielded 0.70 g (83% yield) of 1-methoxy-4-(2-thienyl)naphthalene. Spectroscopic data agree with those reported previously.[19]

2-(4-Methoxyphenyl)-5-(4-methoxynaphthyl)thiophene (Me_2L^5). To a solution of 1-methoxy-4-(2-thienyl)naphthalene (0.35 g, 1.5 mmol) in thf (15 cm^3) at 0 °C under N_2 was added dropwise *n*-BuLi (1.5 mmol; 0.9 cm^3 of a 1.6 M solution in hexane). The mixture was stirred at 0 °C for 1 h and then added to a solution of dry zinc(II) bromide (0.33 g, 1.5 mmol) in thf (5 cm^3) at 0 °C. This mixture was stirred at room temperature for 1 h, and then added to a solution of 4-iodoanisole (0.35 g, 1.3 mmol) and $[PdCl_2(PPh_3)_2]$ (0.045 g, 0.06 mmol) in thf (20 cm^3). After stirring for 2.5 h, the solvent was removed using a rotary evaporator and the residue purified by column chromatography on silica eluting with a 1 : 5 diethyl ether–hexane mixture, to give 0.32 g (70%) of Me_2L^5. EI MS: m/z 346 (M^+, 100%), 331 ($[M–Me]^+$, 80%). ^{1}H NMR (270 MHz, $CDCl_3$): δ 3.84 (3 H, s, $MeOC_6H_4$), 4.03 (3 H, s; $MeOC_{10}H_6$), 6.84 (1 H, d, $J = 8$; naphthyl), 6.93 (2 H, d, $J = 9$ Hz; phenyl), 7.12 (1 H, d, $J = 4$; naphthyl), 7.25 (1 H, d, $J = 4$ Hz; naphthyl), 7.49–7.60 (5 H, m; aromatic CH), 8.25–8.35 (2H, m, aromatic CH).

2-(4-Hydroxyphenyl)-5-(4-hydroxynaphthyl)thiophene (H_2L^5). A mixture of pyridine (10 cm^3) and conc. hydrochloric acid (10 cm^3) was stirred together in an open flask under a steady flow of nitrogen at 200 °C for 1 h. As soon as solid pyridinium chloride started to sublime around the neck of the flask, Me_2L^5 (0.20 g, 0.58 mmol) was added and the mixture stirred under N_2 at 200 °C for 2 h. After cooling to room temperature, water (50 cm^3) was added and the resulting precipitate was collected by filtration. The collected solid was then purified by flash column chromatography on silica eluting with ethyl acetate–hexane (1 : 4) to give pure H_2L^5 as pale yellow microcrystals (97 mg, 53%). EI MS: m/z 318 (M^+, 100%). ^{1}H NMR (270 MHz, $(CD_3)_2CO$): δ 6.92 (2H, d, $J = 9$ Hz; C_6H_4), 7.03 (1H, d, $J = 5$ Hz; $C_{10}H_6$), 7.14 (1H, d, $J = 4$ Hz; $C_{10}H_6$), 7.33–7.59 (6H, m, Ar), 8.23–8.37 (2H, m, Ar).

2,5-Bis(4-methoxynaphthyl)thiophene (Me_2L^6). 2,5-Bis(tri-*n*-butylstannyl)thiophene (1.16 g, 1.75 mmol) and 1-methoxy-4-iodonaphthalene (1.0 g, 3.52 mmol) were dissolved in tetrahydrofuran (20 cm^3). $[PdCl_2(PPh_3)_2]$ (0.125 g, 0.178 mmol) was added and the mixture was then stirred at reflux for 20 h. After cooling to room temperature, the solvent was removed *in vacuo* and the residue purified by column chromatography on silica eluting with hexane. Removal of the solvent afforded Me_2L^6 as a pale yellow powder (0.33 g, 47%). EI MS: m/z 396 (M^+, 100%), 381 ($[M - Me]^+$, 70%), 366 ($[M - 2Me]^+$, 30%). ^{1}H NMR (270 MHz, $CDCl_3$): δ 4.06 (6H, s; Me), 6.88 (2H, d, $J = 8$ Hz; naphthyl), 7.24 (2H, s; thienyl), 7.52–7.61 (6H, m; naphthyl), 8.36 (4H, m; naphthyl).

2,5-Bis(4-hydroxynaphthyl)thiophene (H_2L^6). This was prepared by demethylation of Me_2L^6 using exactly the same procedure as described above for H_2L^5. From 160 mg of 1,4-$MeOC_{10}H_6(2\text{-}C_4H_4S)$-1,4-$C_{10}H_6OMe$, yield was 100 mg (68%). EI MS: m/z 368 (M^+, 100%). ^{1}H NMR (270 MHz, $(CD_3)_2CO$): δ 7.02 (2H, d, $J = 8$ Hz; naphthyl), 7.29 (2H, s; thienyl), 7.51–7.63 (6H, m; naphthyl), 8.32–8.38 (4H, m; naphthyl), 9.36 (2H, br s; OH).

Syntheses of complexes

All complexes were prepared by the same general method. A typical example is given below.

Synthesis of 1. A mixture of 1-naphthol (60 mg, 0.42 mmol) and triethylamine (0.5 cm^3) was stirred in toluene (10 cm^3) for 10 min at reflux. $[Mo(Tp^*)(O)Cl_2]$ (0.15 g, 0.31 mmol) was added and the mixture was then stirred at reflux for a further 2 h. The solvent was then removed using a rotary evaporator and the residue purified by column chromatography on silica eluting with 1 : 1 dichloromethane–hexane. Yield was 110 mg

(60%). Characterisation data for **1** and all other complexes are summarised in Table 1.

Acknowledgements

We thank the EPSRC for financial support. M. D. W. is the Royal Society of Chemistry Sir Edward Frankland fellow for 2001/2002.

References

1 J. A. McCleverty and M. D. Ward, *Acc. Chem. Res.*, 1998, **31**, 842.
2 S. Bayly, J. A. McCleverty, M. D. Ward, D. Gatteschi and F. Totti, *Inorg. Chem.*, 2000, **39**, 1288; V. A. Ung, S. M. Couchman, J. C. Jeffery, J. A. McCleverty, M. D. Ward, F. Totti and D. Gatteschi, *Inorg. Chem.*, 1999, **38**, 365; A. Bencini, D. Gatteschi, J. A. McCleverty, D. N. Sanz, F. Totti and M. D. Ward, *J. Phys. Chem. A*, 1998, **102**, 10545; V. A. Ung, D. A. Bardwell, J. C. Jeffery, J. P. Maher, J. A. McCleverty, M. D. Ward and A. Williamson, *Inorg. Chem.*, 1996, **35**, 5290; V. A. Ung, A. M. W. Cargill Thompson, D. A. Bardwell, D. Gatteschi, J. C. Jeffery, J. A. McCleverty, F. Totti and M. D. Ward, *Inorg. Chem.*, 1997, **36**, 3447; J. Hock, A. M. W. Cargill Thompson, J. A. McCleverty and M. D. Ward, *J. Chem. Soc., Dalton Trans.*, 1996, 4257; A. M. W. Cargill Thompson, D. Gatteschi, J. A. McCleverty, J. A. Navas Badiola, E. Rentschler and M. D. Ward, *Inorg. Chem.*, 1996, **35**, 2701.
3 S. R. Bayly, E. R. Humphrey, H. de Chair, C. G. Paredes, Z. R. Bell, J. C. Jeffery, J. A. McCleverty, M. D. Ward, F. Totti, D. Gatteschi, S. Courric and C. G. Screttas, *J. Chem. Soc., Dalton Trans.*, 2001, 1401.
4 N. C. Harden, E. R. Humphrey, J. C. Jeffery, S.-M. Lee, M. Marcaccio, J. A. McCleverty, L. H. Rees and M. D. Ward, *J. Chem. Soc., Dalton Trans.*, 1999, 2417.
5 R. Kowallick, A. N. Jones, Z. R. Reeves, J. C. Jeffery, J. A. McCleverty and M. D. Ward, *New J. Chem.*, 1999, **23**, 915.
6 S.-M. Lee, M. Marcaccio, J. A. McCleverty and M. D. Ward, *Chem. Mater.*, 1998, **10**, 3272.
7 A. McDonagh, S. R. Bayly, D. J. Riley, M. D. Ward, J. A. McCleverty, M. A. Cowin, C. N. Morgan, R. Varrazza, R. V. Penty and I. H. White, *Chem. Mater.*, 2000, **12**, 2523.
8 R. J. Mortimer, *Chem. Soc. Rev.*, 1997, 147; R. J. Mortimer, *Electrochim. Acta*, 1999, **44**, 2971; *Integrated Optical Circuits and Components: Design and Applications*, ed. E. J. Murphy, Marcel Dekker, New York, 1999.
9 W. E. Cleland, Jr., K. M. Barhhart, K. Yamanouchi, D. Collison, F. E. Mabbs, R. B. Ortega and J. H. Enemark, *Inorg. Chem.*, 1987, **26**, 1017.
10 A. I. Vogel, *Textbook of Practical Organic Chemistry*, Longman, London and New York, 4th edn., 1978, p. 715.
11 J. M. Tedder and B. Webster, *J. Chem. Soc.*, 1960, 4417.
12 J. C. Jeffery, E. Schatz and M. D. Ward, *J. Chem. Soc., Dalton Trans.*, 1992, 1921; B. M. Holligan, J. C. Jeffery, M. K. Norgett, E. Schatz and M. D. Ward, *J. Chem. Soc., Dalton Trans.*, 1992, 3345; B. M. Holligan, J. C. Jeffery and M. D. Ward, *J. Chem. Soc., Dalton Trans.*, 1992, 3337.
13 E. Negishi, *Acc. Chem. Res.*, 1982, **15**, 340.
14 S.-M. Lee, R. Kowallick, M. Marcaccio, J. A. McCleverty and M. D. Ward, *J. Chem. Soc., Dalton Trans.*, 1998, 3443.
15 Chem3D Pro version 3.5.1, CambridgeSoft corporation, Cambridge, MA, USA, 1997.
16 A. M. McDonagh, M. P. Cifuentes, N. T. Lucas, M. G. Humphrey, S. Houbrechts and A. Persoons, *J. Organomet. Chem.*, 2000, **505**, 193.
17 H. O. Wirth, O. Königstein and W. Kern, *Justus Liebigs Ann. Chem.*, 1960, **634**, 84.
18 D. E. Seitz, S. H. Lee, S. H. Hanson and J. C. Bottaro, *Synth. Commun.*, 1983, **13**, 121.
19 T. Sone, R. Yokoyaya, Y. Okuyama and K. Sato, *Bull. Chem. Soc. Jpn.*, 1986, **59**, 83.